

## Zirconium oxide nanoparticles: Fabrication, study and application for removal of organic dye from aqueous media

N.E.Marghany, M.M.Moustafa, A.M. El-Sharkawy and A.A.Ali

Chemistry Department, Faculty of Science, Benha University, Benha, Egypt

E-mail: nada\_chemist@yahoo.com,

### Abstract

Herein, the prepared zirconium oxide ( $ZrO_2$ ) nanoparticles were fabricated using the auto-combustion method and glutamic, succinic and tartaric acids as organic fuels. The obtained zirconium oxide samples were calcinated at  $600\text{ }^\circ\text{C}$  for 1 hour. The synthesized zirconium oxide nanoparticles (ZONPs) were characterized using (XRD) X-ray diffraction, and (FTIR) Fourier transform infrared spectroscopy. The crystallite sizes of the obtained samples were calculated. The synthesized zirconium oxide nanoparticles (ZONPs) used as adsorbents for organic dye from water. The adsorption capacity of the zirconium oxide nanoparticles was studied utilizing various factors. The adsorption kinetic and adsorption isotherm models are used for the interpretation of the organic dye removal on the fabricated zirconium oxide nanoparticles as adsorbents.

**Keywords:** Auto-combustion method, Zirconium oxide nanoparticles, XRD, organic dye.

### 1. Introduction

Water is considered polluted when it gets any change in its quality, composition either naturally or due to the human activities. Water become inappropriate for drinking, industrial, agricultural, domestic, wildlife, recreational and other uses as result of the present of pollution. Wastewater is obtained according to the presence of different kinds of pollutants such as organic dyes and heavy metals, which deserves more significant attention [1-5].

During the previous century, huge volumes of organic pigments have been loosed into the environment media as a result of the ongoing expansion of various industries on our planet, such as the dyeing and printing industrialization process. Dyes are common every day chemical compounds that are commonly used in a lot of fields to color their products [6] including leather, rubber, paper, textile, plastics, printing, etc. Chemical structure, color, application, and particle charge in a solution can all be used to classify dyes. Generally, Dyes are divided into two categories: natural dyes and synthetic dyes. Animal and mineral dyes are the most common sources of natural dyes. On the other hand, due to the improvement of industrial activities, natural dyes could not cover the people's requirements. As a result, synthetic dyes have been produced and have steadily supplanted natural dyes in the fabric and textile sectors. Synthetic dyes, both ionic and non-ionic, are commonly used. Ionic dyes are divided into two categories: anionic dyes like (reactive, acid and direct dyes), and cationic dyes. Non-ionic dyes classified into vat and disperse dyes. In addition to that categorization, dyes classified by their chemical structure are particularly common such as azo, Nitro, Nitroso, Anthraquinone, Indigoid, and Triarylmethane dyes [7, 8].

Acid Violet 19 is an acidic dye with chemical formula,  $C_{20}H_{17}N_3Na_2O_9S_3$ . It is one of the dyes used in Masson's trichrome stain and is widely used in histology. It can also be used to identify germs that are growing. It can also be used to identify growing microorganisms. Also, it has carcinogenic and toxic properties, more careful treatment is required before discharging. Carcinogenicity, mutagenicity, and dysfunction of a human kidney, liver,

beings, brain, reproductive system and central nervous system are all caused by dyes molecules in wastewater [8, 9]. However, the side effects of dyes that discovered by scientists and practically all chemical, physical and biological methods are being used in dyeing wastewater treatment including oxidation, advanced oxidation process, adsorption, coagulation, flocculation, membrane separations, ion-exchange, electrochemical process, photocatalysis, biodegradation, etc. Among them, adsorption techniques come to the fore due to their low cost, ease of use and the more efficient adsorbent design [6, 10].

Nanomaterials have unusual physicochemical properties, due to their small size and high surface-area and these materials are viewed differently than their bulk material [11, 12]. Between these nanomaterials, zirconium oxide is an example of simple oxide with the chemical formula ( $ZrO_2$ ), occasionally, Zirconia is the name for it. It's a zirconium oxide that's white and crystalline. Zirconium oxide is a commonly used inorganic substance that is chemically stable, non-toxic and water insoluble. As a result, it could be an appealing choice for purifying drinking water. Due to its chemical and thermal stability, as well as good mechanical features such as high strength and fracture toughness, high melting point, high corrosion resistance, and low thermal conductivity, it is extremely important [13, 14]. It is utilized in various of applications like sensing, catalysis, paint, coatings, wastewater treatment, fuel cells and advanced ceramic [15, 16]. The main objective of this work prepared and characterized zirconium oxide nanoparticles and it used as adsorbent for the removal of acid violet 19 (AV19) dye from aqueous media. The adsorption isotherm and kinetic models were investigated.

### 2. Experimental

#### 2.1. Chemicals and reagents

Zirconium oxychloride (octahydrate) ( $ZrOCl_2 \cdot 8H_2O$ ; 99%) was purchased from Research-Lab Chemical Industries, India. L-Glutamic acid (GA:  $C_5H_9O_4N$ ; 99%) was purchased from Noreshark fine Chemicals Company, Egypt, succinic acid (SA:  $C_4H_6O_4$ ; 99%) was purchased from Qualikems fine chemicals company, India. Tartaric

acid (TA: C<sub>4</sub>H<sub>6</sub>O<sub>6</sub>; 99%), nitric acid (HNO<sub>3</sub>; 70%) and ammonium hydroxide (NH<sub>4</sub>OH; 25%) were supplied by El-Nasr Pharmaceutical Chemical Company, Egypt. Acid violet 19 dye (C<sub>20</sub>H<sub>17</sub>N<sub>3</sub>Na<sub>2</sub>O<sub>9</sub>S<sub>3</sub>, molecular weight: 585.54 g/mol, λ=546 nm) was obtained from Oxford Lab Chem Company, India. The used materials (chemicals and reagents) in the experimental part were of analytical grade and used as obtained without any treatment. Freshly bidistilled water was used through all experiments. The chemical structure of Acid Violet 19 is depicted in the Fig (1).

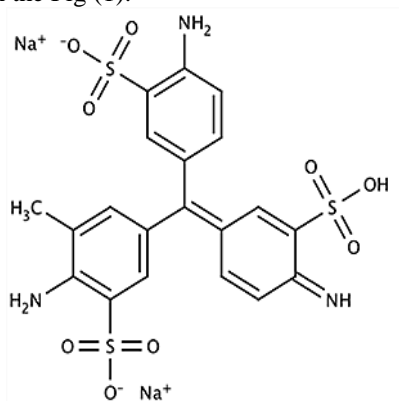


**Fig. (1) Structure of acid violet 19 dye.**

## 2.2. Preparation of zirconium oxide nanoparticles (ZONPs)

Zirconium oxychloride (0.02 mol, 6.445 g) was dissolved in 50 mL of bidistilled water and then the pH of solution adjusted to become 9 by the adding of NH<sub>4</sub>OH solution. The obtained white precipitated was separated and washed several times. The obtained precipitated was dissolved again in distilled water and the calculated volume of nitric acid with continuous stirring till it forms the clear solution. The obtained solutions were mixed with solutions of different weights of succinic acid (SA), glutamic acid (GA) and tartaric acid (TA) fuels, separately. The calculated moles of organic fuels according to equations 1, 2, and 3. The obtained solutions magnetically stirred on hotplate at 150°C until gels were obtained. The obtained gels were ignited at 250°C and the ashes powder were fabricated. The as-synthesized ashes were calcinated at 600°C for 1 h and the fine and crystalline zirconium oxide nanoparticles were fabricated. The product names, starting material for the synthesis of zirconium oxide nanoparticles using succinic acid, glutamic acid and tartaric acid fuels are outlined in Table 1.

**Table (1)** sample name and starting material composition in the fabrication of zirconium oxide nanoparticles (ZONPs)

No	Sample names	Zr salt, mole	Fuel, mole	Fuel, g	Zr/fuel, molar ratio
1	ZSA	0.02	SA	1.7	1:1.4
2	ZGA	0.02	GA	1.4	1:2.1
3	ZTA	0.02	TA	3	1:1

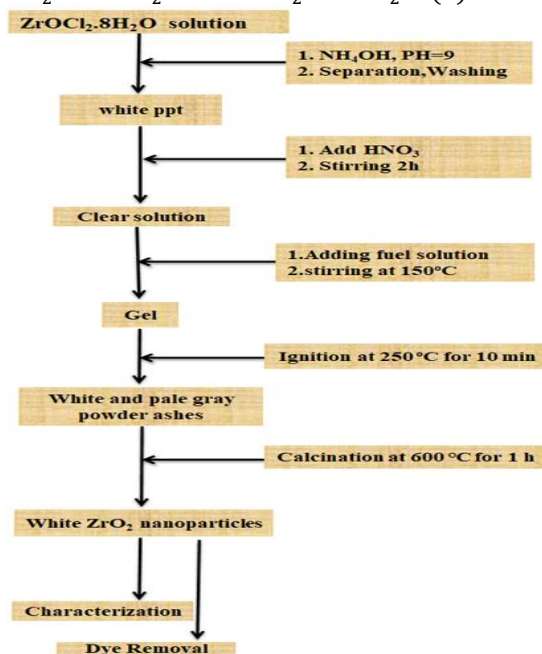
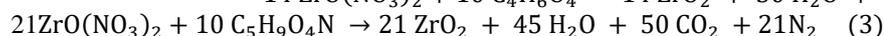
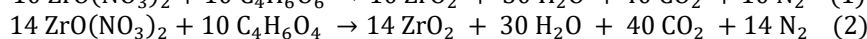
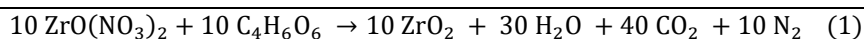


**Fig. (2)** Schematic flowchart for the preparation of zirconium oxide nanoparticles (ZONPs) using the combustion process and different organic fuels.

**2.3. Characterization tools**

The obtained ZGA, ZSA and ZTA samples were recorded using (Thermo Scientific; model Nicolet IS10) an FTIR spectrometer at the room temperature from 4000 to 400 cm<sup>-1</sup>. The appeared phase of the calcined ZGA, ZSA and ZTA samples was tested by the recording of the XRD patterns using (Bruker; model D 8 advance) 18 KW diffractometer with monochromatic Cu-Ka radiation, 1.54178 (Å) in the angular range of 10-80° with step size 0.02° (2θ) and scan step time 0.4 (s). The adsorption process was investigated using (Jasco; model V 670) a Jasco UV-Vis spectrophotometer

**3. Results and Discussion**

**3.1. Characterization of the fabricated zirconium oxide nanoparticles (ZONPs)**

Using an X-ray diffraction tool, the phase composition and crystallite sizes of the obtained ZrO<sub>2</sub> nanoparticles were studied. XRD patterns of the zirconium oxide (ZGA, ZSA and ZTA samples) after the production using combustion method and calcination at 600°C for one hour are shown in Fig (2). According to the XRD patterns after the calcination at 600°C, the presence of the sharp

diffraction peaks in their diffraction patterns reflected the presence the fine of zirconium oxide nanoparticles as shown in Fig(3). No peaks of other phases were found in the XRD pattern, indicating that the crystalline ZrO<sub>2</sub> nanoparticles obtained by the combustion method and different organic fuels (glutamic, succinic and tartaric) acids. Also, the collected data from XRD patterns revealed that the obtained zirconium oxide crystallized in Tetragonal(T) system for all samples according to Reference code No. 01-088-1007 (crystal lattice: a=b=3.5984 Å and c=5.1520 Å and crystal angle: α=B=γ=90°)[17]. Only ZSA sample appeared the second phase for zirconium oxide in the form of Monoclinic(M) system according to Reference code No. 01-088-2390(crystal lattice: a= 5.1501 Å, b=5.2077 Å and c=5.3171 Å and crystal angle: α=γ=90° and B=99.2240°). The crystallite size (Z, nm) of the ZrO<sub>2</sub> nanoparticles can extracted by using the Scherrer equation (4):

$$Z = D\lambda / \beta \cos\theta_B \quad (4)$$

Where, λ the X-ray radiation wavelength, D is constant, β is (FWHM) the full width at half maximum of the diffraction peak and θ<sub>B</sub> is the Bragg diffraction angle.

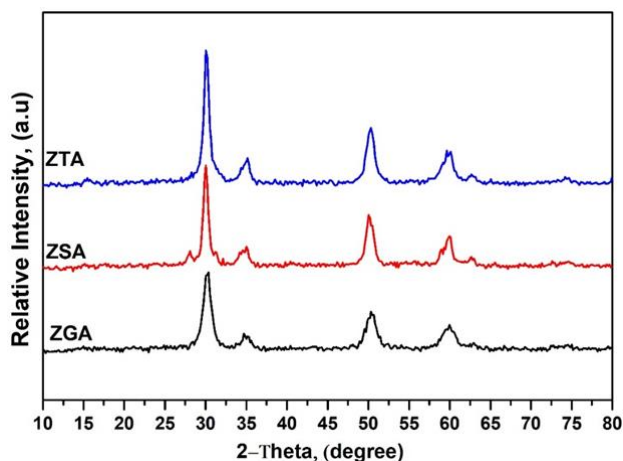


**Fig. (3)** XRD of zirconium oxide nanoparticles (ZGA, ZSA and ZTA samples) using combustion method and different organic fuels.

**Table (2) the average crystallite sizes for ZrO<sub>2</sub> nanoparticles.**

No.	Sample name	Crystallite size, (nm)	ZrO <sub>2</sub> phases
1	ZGA	10	(T, 100%)
2	ZSA	12	(T, 71 %) + (M, 29%)
3	ZTA	9	(T, 100%)

The calcined ZGA, ZSA and ZTA samples were characterized using FTIR spectroscopy as seen in Fig (4). The spectra were detected over the range of 400 - 4000 cm<sup>-1</sup> to identify the function groups inside the synthesized ZGA, ZSA and ZTA samples which confirm the structure of the obtained zirconium oxide. In all spectra, there were peaks at 3500 cm<sup>-1</sup>, 3300 cm<sup>-1</sup> and 3400 cm<sup>-1</sup> referred to the presence of stretching vibrations of the hydroxide groups or/and the adsorbed H<sub>2</sub>O molecules on the surface of zirconium oxide nanoparticles(ZGA, ZSA and ZTA samples). Besides, the peaks in the 1630-1650 cm<sup>-1</sup> range are pointed to the vibrational modes of the bending of the hydroxide groups on the zirconium oxide surface for ZGA, ZSA and ZTA samples. The peak at 1020-1050 cm<sup>-1</sup> referred to the C-O, and C-N with the fabricated samples. The peaks observed at 450-500 cm<sup>-1</sup> for the calcined samples are confirm to the presence of the tetragonal structure of ZrO<sub>2</sub> stretching vibration modes

of inside the lattice of the zirconium oxide nanoparticles. The shoulder at  $550\text{cm}^{-1}$  and  $700\text{cm}^{-1}$  are related to the monoclinic structure of  $\text{ZrO}_2$  stretching vibration modes

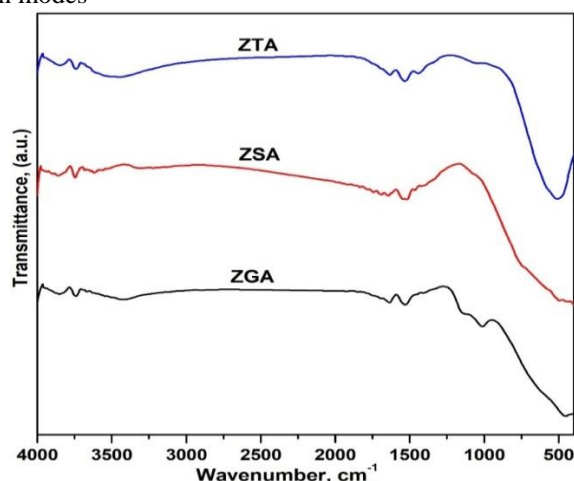


Fig.(4) FTIR of zirconium oxide nanoparticles (ZGA, ZSA and ZTA samples) using combustion method and different organic fuels.

### 3.2. Adsorption studies

The synthesized samples were utilized as adsorbents to rapidly remove acid violet19 dye from the aqueous media using batch mode. Different adsorption parameters including pH, contact time, initial dye concentrations, and an adsorbent dosage, were studied to determine the adsorption properties of the synthesized product. To obtain the desired concentrations, dye solutions were synthesized by dissolving the dye under study in deionized water. The observed and starting dye concentrations were used to calculate uptake values. The obtained data from batch mode were utilized to determine ( $q_e$ ) the adsorption capacity and (R %) the removal efficiency [18] from equation No.5 and 6, respectively.

$$q_e = \frac{(C_o - C_t)V}{w} \quad (5)$$

$$\text{Removal (R\%)} = \frac{(C_o - C_t)}{C_o} \times 100 \quad (6)$$

Where,  $q_e$  is the uptake of dye at certain time in (mg/g), V represents the volume of the solution in (L),  $C_o$  represents the starting dye concentration in (mg/L),  $C_t$  represents the concentration of dye at time t in (mg/L), and w is the adsorbent's weight in (g).

#### 3.2.1. Effect of initial pH

One of the most critical variables which controlling the adsorption process particularly the adsorption capacity, is the pH of the adsorbate solution. The effect of initial pH for the removal of 100 mg/L of acid violet19 dye over 50 mg of  $\text{ZrO}_2$  nanoparticles (ZGA sample) was studied in the pH range from 1.5 to 8. The removal efficiency of the dye was measured at  $\lambda_{\text{max}} = 546$  nm, and it attained its maximum values at this wavelength (70%) at pH = 6. The removal efficiency increased by raising of the pH values for ZGA sample under study, followed by the decreasing after pH=6. The removal dye efficiency was determined for ZGA samples as shown in (Fig 5, a).

#### 3.2.2. Effect of contact time

The contact time between adsorbent and adsorbate is considered one of the most essential factors impacting on the adsorption process performance. The effect of contact time on the adsorption of acid violet 19 dye over  $\text{ZrO}_2$  nanoparticles (ZGA sample) was investigated at pH 6, 0.05 g adsorbent dose and initial acid violet19 dye concentration of 50 mg/L. (Fig 5, b) shows the adsorption capacity of ZGA sample for the removal of the acid violet19 dye as a relation of stirring times ranging between 1 - 180 min. The maximum removal of the dye (R=84.5%) was attained in 150 min and the absorption capacity recorded 21mg/g.

#### 3.2.3. Effect of adsorbent dose

The adsorbent dose is one of the most important parameters that can define an adsorbent's capacity for a given initial concentration of adsorbate. The effect of adsorbent dosage for the adsorption of acid violet19 dye studied by adding different amounts of the adsorbent in range (0.01–0.1g) and the pH of the solutions were fixed at 6. The adsorbent was added into a 25 mL dye solution with a 50 mg/L starting concentration. After equilibrium time, the solutions were centrifuged and analyzed for the dye separation as depicted in (Fig 5, c). The extracted results revealed that increasing adsorbent dosage increases removal efficiency of the dye due to an increase in the number of active sites on the adsorbent surface.

#### 3.2.4. Effect of initial dye concentration

One of the most critical parameters that can influence the adsorption process is the initial dye concentration. The impact of various initial concentration of acid violet19 dye between 10 and 100 mg/L. Adsorption experiments were applied at pH =6 and 0.05 g adsorbent dose. After 150 min of stirring, UV-Vis spectrophotometric was used to measure the remaining concentration of dye in the supernatant after the adsorbent was isolated by centrifugation. The adsorption capacities were calculated from the data that was extracted. The relation between loading capacity and initial dye concentration is presented

in (Fig5, d)from the extracted data, increase of initial dye concentration results in a corresponding dye removal capacity till 100 mg/L as a starting concentration.

Maximum adsorption capacity for acid violet 19 dye over ZGA sample determined to be 31 mg/g after 150 min.

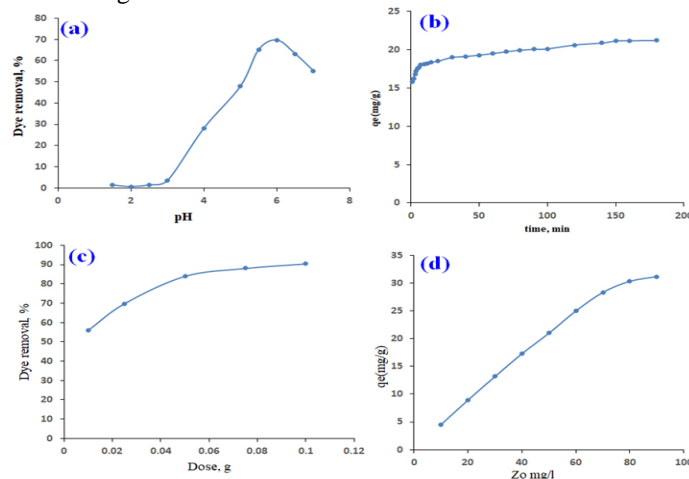


Fig. (5) Effect of pH (a), time (b), adsorbent dose (c) and initial concentration (d) for the removal of the acid violet 19 dye using the zirconium oxide nanoparticle (ZGA sample).

4. Adsorption kinetics

The study of adsorption kinetics is crucial for predicting the rate at which a pollutant can be removed from aqueous solutions and understanding the mechanism of adsorption events. With time, the adsorption capacity of the ZGA sample raised to its maximum. Kinetic factors of the removal acid violet19 dye on ZGA sample were estimated using pseudo-first order, pseudo-second-order equations and intra-particle diffusion model [17-21] as presented in the following equations No. 7, 8 and 9. Through to the computation of kinetic factors, the relationships were used to get information about the adsorption process rate and adsorbate quantity as shown in the following Figure6. The kinetic parameters calculated from relations and summarized in Table3.

$$\log(q_e - q_t) = \log(q_e) - \frac{K_1}{2.303} t \quad (7)$$

$$\frac{t}{q_t} = \frac{1}{K_2 q_e^2} + \frac{t}{q_e} \quad (8)$$

$$q_t = K_i t^{0.5} + C \quad (9)$$

Where,  $q_e$  and  $q_t$  are the dye adsorbed quantities (mg/g) at equilibrium and time  $t$  (min), respectively.  $t$  (min) is contact time.  $k_1$  is pseudo-first-order adsorption rate constant ( $\text{min}^{-1}$ ) and  $k_2$  ( $\text{g}/\text{mg}\cdot\text{min}$ ) is pseudo-second-order adsorption rate constant.  $k_i$  is intra-particle diffusion constant ( $\text{mg}/\text{g}\cdot\text{min}^{0.5}$ ), and  $C$  is the thickness of boundary

layer (mg/g).According to the plot of  $\log(q_e - q_t)$  against  $t$  for pseudo-first-order model (Figure6, a), the plot  $t/q_t$  against time  $t$  for pseudo-second-order model(Figure 6, b) and the plot of  $qt$  vs. square root of time for intra-particle diffusion (Figure 6, c) as represented in Fig (6). The extracted data from Figure 6 summarized in Table 1. The pseudo-second-order model is better suited for the removal of acid violet19 dye on the synthesized zirconium oxide nanoparticles based on the  $R^2$  values, ( $r^2=0.998$ ) than the pseudo first order. Finally, the removal of the acid violet19dye follows the pseudo-second-order model, and the theoretical adsorption capacity calculated ( $q_e=21.16$ ) is very similar to the experimental one ( $q_e=21.22$ ).If intra-particle diffusion is the rate limiting step, should be a direct line passing through the origin with  $C = 0$ . The straight line does not pass the origin, indicating that overall adsorption process may be mediated by multiple mechanisms including bulk diffusion, etc. Intra-particle diffusion cannot be used for the rate determining step for the removal of acid violet19 dye on the synthesized zirconium oxide nanoparticles (ZGA sample). Table3 shows the extracted values for  $K_i$  and  $C$  where is obtained that the line does not pass through the origin, and it is illustrated that the intra particle diffusion is not the only model for explaining the dye removal mechanism.

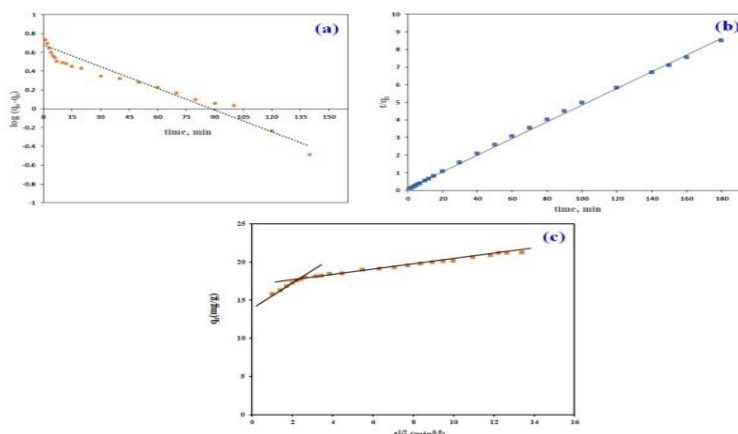


Fig. (6) Pseudo-first-order (a), pseudo-second-order (b) and intra-particle diffusion (c) models for an adsorption of acid violet19 dye on ZGA sample.

Table (3) Adsorption kinetic parameters of the removal of acid violet 19 dye on zirconium oxide nanoparticles (ZGA sample).

Kinetic parameters	Parameter	Values
<b>Pseudo first order</b>	$K_1(\text{min}^{-1})$	0.02448
	$q_m(\text{cal})(\text{mg/g})$	5.62
	$R^2$	0.8092
	$q_m(\text{exp})(\text{mg/g})$	21.22
<b>Pseudo second order</b>	$K_2(\text{g/mg}\cdot\text{min})$	0.020034
	$q_m(\text{cal})(\text{mg/g})$	21.16
	$R^2$	0.9989
	$q_m(\text{exp})(\text{mg/g})$	21.22
<b>Intra-particle diffusion</b>	$K_i(\text{mg/g}\cdot\text{min}^{0.5})$	1.379
	$C(\text{mg/g})$	14.399
	$R^2$	0.9938
	$K_i(\text{mg/g}\cdot\text{min}^{0.5})$	0.3147
	$C(\text{mg/g})$	17.128
	$R^2$	0.9419

5. Adsorption isotherms studies

The adsorption isotherms models were tested via study of the relation of the adsorption capacities and several initial concentrations of acid violet 19 dye (10 and 100 mg/L) for ZGA sample. The experimental data was described using Langmuir and Freundlich isotherm models with varied equilibrium concentrations of acid violet 19 (10 and 100 mg/L) for ZGA sample utilising 0.05 gram of zirconium oxide nanoparticles at pH=6 and 293 K. The equations of Langmuir, Freundlich and Temkin[17-21] are showed in No. 10, 11 and 12 respectively.

$$\frac{Z_e}{q_e} = \frac{1}{K_L q_m} + \frac{Z_e}{q_m} \tag{10}$$

$$\ln q_e = \ln K_F + \frac{1}{n} \ln Z_e \tag{11}$$

$$q_e = Y \ln K_T + Y \ln Z_e \tag{12}$$

Where,  $Z_e$  is the acid violet 19 dye equilibrium concentration in the solution (mg/L),  $q_e$  is the acid violet 19 dye equilibrium adsorption capacity on the adsorbent,  $K_L$  is the Langmuir parameter (L/mg),  $q_m$  is the maximum quantity of adsorbed solute to the adsorbent (mg/g),  $K_F$  represent the Freundlich constant (mg/g) and  $(1/n)$  is the heterogeneity factor.  $K_T$  is the equilibrium binding constant (L/mol) corresponding to the maximum binding energy and constant  $Y$  is proportional to the heat of adsorption. The slope and intercept used for the determination of the

Langmuir isotherm constants from a plot of  $Z_e/q_e$  versus  $Z_e$  as seen in (Fig 7, a).The slope and intercept used for the calculation of the Freundlich isotherm constants from a plot of  $\ln q_e$  versus  $\ln Z_e$  as shown in (Fig 7, b).The slope and intercept determined the isotherm constants from a plot of  $q_e$  versus  $\ln Z_e$  as shown in (Fig 7, c).

From  $R^2$  values, the Langmuir model of the acid violet 19dye adsorption on the ZGA sample fits the data better than the other models. It signifies that the removal of acid violet 19dye from the  $ZrO_2$  nano-adsorbent (ZGA sample) in the of monolayer without any contact between adsorbed molecules. The theoretical and experimental of adsorption capacity calculated from Langmuir model to be 38 mg/g and 31 mg/g. Table 4 is summarized the parameters were extracted from Langmuir, Temkin and Freundlich models.  $R_L$  values were calculated to be 0.38436-0.05877 which is related to the starting concentration 10-100 mg/g. these values explain that an adsorption process of the acid violet 19 dye on the ZGA sample is a favorable adsorption process. According to the value of  $b$  parameter from Temkin model, the heat of adsorption ( $b$ ) calculated to be 0.291 KJ/mole and it explain the weak interaction force between  $ZrO_2$  and acid violet 19dye.

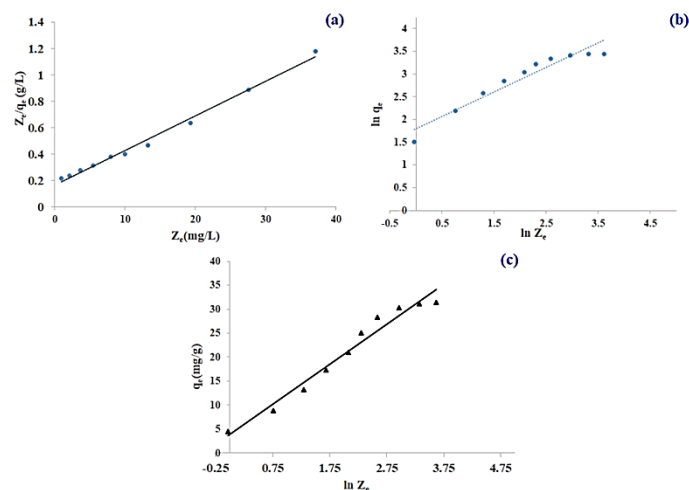


**Fig. (7)** Langmuir (a), Freundlich (b) and Temkin (c) models for removal the acid violet 19 dye on zirconium oxide nanoparticles (ZGA sample).

**Table (4)** The obtained parameters from Langmuir, Freundlich and Temkin isotherms for  $ZrO_2$  adsorbent (ZGA samples).

Adsorption isotherm	Parameter	Values
		ZGA
Langmuir	$K_L$ (L/mg)	0.160171
	$q_m$ (cal) (mg/g)	38.00
	$R_L$	0.05877-0.38436
	$R^2$	0.9921
	$q_m$ (exp) (mg/g)	31.00
Freundlich	$K_F$ [(L/mg) (L/mg) $^{1/n}$ ]	6.0454
	$q_m$ (cal) (mg/g)	63.6
	$n$ (L/mg)	1.863
	$R^2$	0.9237
	$q_m$ (exp) (mg/g)	31.00
Temkin	$K_T$ (L/mg)	1.5971
	$b$ (J/mol)	291
	$Y$	3.9175
	$R^2$	0.9687

#### 4. Conclusions

Zirconium oxide nanoparticles were fabricated via combustion method, then calcination at 600 °C for 1 h. The obtained samples were characterized by employing various techniques. The obtained  $ZrO_2$  nano-adsorbent (ZGA sample) crystallized after the calcination with a crystal size calculated to be 9-12 nm. According to FTIR, absorption peaks in the range of 400-600  $cm^{-1}$  are related to the vibration modes of Zr-O band inside  $ZrO_2$  nanoparticles. The optimum adsorption parameters of the acid violet 19 dye on  $ZrO_2$  adsorbent (ZGA sample) been investigated using a batch technique. A maximum adsorption capacity for the acid violet 19 dye over ZGA sample determined to be 31 mg/g. The separation results were well fitted with Langmuir adsorption isotherm and the pseudo-second-order.

#### Acknowledgements

The authors are grateful to Benha University, Egypt for their assistance with this study.

#### References

- [1] P. Goel, Water pollution: causes, effects and control, New Age International 2006.

- [2] R. Ramanath, W.E. Snyder, Y. Yoo, M.S.J.I.S.P.M. Drew, Color image processing pipeline, 22 (2005) 34-43.
- [3] A.A. Ali, I.S. Ahmed, A.S. Amin, M.M. Gneidy, Auto-combustion Fabrication and Optical Properties of Zinc Oxide Nanoparticles for Degradation of Reactive Red 195 and Methyl Orange Dyes, J. Inorg. Organomet. Polym Mater. 31 (2021) 3780-3792.
- [4] A.A. Ali, E.A. El Fadaly, N.M. Deraz, Auto-combustion fabrication, structural, morphological and photocatalytic activity of CuO/ZnO/MgO nanocomposites, Mater. Chem. Phys. 270 (2021) 124762.
- [5] A.A. Ali, I.S. Ahmed, E.M. Elfiky, Auto-combustion Synthesis and Characterization of Iron Oxide Nanoparticles ( $\alpha$ -Fe $2O_3$ ) for Removal of Lead Ions from Aqueous Solution, J. Inorg. Organomet. Polym Mater. 31 (2021) 384-396.
- [6] Y. Zhou, J. Lu, Y. Zhou, Y.J.E.p. Liu, Recent advances for dyes removal using novel adsorbents: a review, 252 (2019) 352-365.

- [7] T. Ngulube, J.R. Gumbo, V. Masindi, A.J.J.o.e.m. Maity, An update on synthetic dyes adsorption onto clay based minerals: A state-of-art review, 191 (2017) 35-57.
- [8] M.T. Yagub, T.K. Sen, S. Afroze, H.M.J.A.i.c. Ang, i. science, Dye and its removal from aqueous solution by adsorption: a review, 209 (2014) 172-184.
- [9] R.S. Aliabadi, N.O.J.J.o.c.p. Mahmoodi, Synthesis and characterization of polypyrrole, polyaniline nanoparticles and their nanocomposite for removal of azo dyes; sunset yellow and Congo red, 179 (2018) 235-245.
- [10] A.A. Adeyemo, I.O. Adeoye, O.S.J.A.W.S. Bello, Adsorption of dyes using different types of clay: a review, 7 (2017) 543-568.
- [11] L. Yin, Z. Zhong, Nanoparticles, Biomaterials Science, Elsevier2020, pp. 453-483.
- [12] A.A. Ali, E.M. Elfiky, I.S. Ahmed, A.A. Khalil, T.Y.J.D. Mohamed, W. TREATMENT, Auto-combustion fabrication and characterization of TiO<sub>2</sub> nanoparticles and utilization as an adsorbent for removal of Pb<sup>2+</sup> from aqueous solution, 193 (2020) 83-94.
- [13] H. Cui, Q. Li, S. Gao, J.K.J.J.o.I. Shang, E. Chemistry, Strong adsorption of arsenic species by amorphous zirconium oxide nanoparticles, 18 (2012) 1418-1427.
- [14] L. Li, W.J.S.s.c. Wang, Synthesis and characterization of monoclinic ZrO<sub>2</sub> nanorods by a novel and simple precursor thermal decomposition approach, 127 (2003) 639-643.
- [15] M. Verma, V. Kumar, A.J.M.C. Katoch, Physics, Synthesis of ZrO<sub>2</sub> nanoparticles using reactive magnetron sputtering and their structural, morphological and thermal studies, 212 (2018) 268-273.
- [16] G.-Y. Guo, Y.-L.J.J.o.M.C. Chen, High-quality zirconia powder resulting from the attempted separation of acetic acid from acrylic acid with zirconium oxychloride, 11 (2001) 1283-1287.
- [17] A.A. Ali, S.A. Shama, S.R. EL-Sayed, Fabrication, structural and adsorption studies of zirconium oxide nanoparticles, J Benha Journal of Applied Sciences 5 (2020) 245-253.
- [18] A.A. Ali, S.A. Shama, A.S. Amin, S.R. El-Sayed, Synthesis and characterization of ZrO<sub>2</sub>/CeO<sub>2</sub> nanocomposites for efficient removal of Acid Green 1 dye from aqueous solution, Mater. Sci. Eng., B 269 (2021) 115167.
- [19] A.A. Ali, S.R. El-Sayed, S.A. Shama, T.Y. Mohamed, A.S. Amin, Fabrication and characterization of cerium oxide nanoparticles for the removal of naphthol green B dye, Desalination and Water Treatment 204 (2020) 124-135.
- [20] A. Ali, H. Aly, I. Ahmed, F. Fathi, Sol-Gel Auto-Combustion Preparation and Characterization of Silica Nanoparticles for The Removal of Congo Red Dye from Aqueous Media, J Benha Journal of Applied Sciences 5 (2020) 199-208.
- [21] A. Ali, M. Nassar, S. Shama, A. El Sharkwy, N. El Sayed, Sol-Gel Auto-Combustion Synthesis and Identification of Silicon Dioxide Nanoparticles for The Removal of Sunset Dye from Aqueous Solutions, J Benha Journal of Applied Sciences 5 (2020) 217-229.